Supporting Information

The impacts of molecular adsorption on antiferromagnetic $MnPS_3$ monolayer: Enhanced magnetic anisotropy and intralayer Dzyaloshinskii-Moriya interaction

Ke Wang[1,2], Kai Ren[3], Yuan Cheng[2,4], Shuai Chen[5] and Gang Zhang[5]*

1. School of Automation, Xi'an University of Posts & Telecommunications, Shaanxi, 710121, China
2. Monash Suzhou Research Institute, Monash University, Suzhou Industrial Park, Suzhou 215000, PR China
3. School of Mechanical and Electronic Engineering, Nanjing Forestry University, Nanjing, Jiangsu 210042, China
4. Department of Materials Science and Engineering, Monash University, VIC 3800, Australia
5. Institute of High Performance Computing, A*STAR, 138632, Singapore

*Corresponding authors. Email: zhangg@ihpc.a-star.edu.sg (G.Z.)

Part 1. Adsorption Energy of MPS-molecule system

Table S1. The adsorption energy of MPS-molecule system around the top of Mn ($E_{Ad\text{-}Mn}$), P ($E_{Ad\text{-}P}$) and S ($E_{Ad\text{-}S}$) atoms.

SYSTEM	$E_{Ad\text{-}Mn}$ (eV)	$E_{Ad\text{-}P}$ (eV)	$E_{Ad\text{-}S}$ (eV)
MPS-CO	-0.10248	**-0.10868**	-0.09388
MPS-N_2	**-0.09898**	-0.08331	-0.07231
MPS-NH_3	-0.12942	**-0.21462**	-0.09852
MPS-NO	-0.4389	**-0.4464**	-0.42000
MPS-NO_2	**-0.49202**	-0.45692	-0.44652

As well known, the lowest adsorption energy corresponds to the most stable adsorption configuration. The E_{Ad} of CO molecule adsorbed above P atom is 6.2 and 14.8 meV lower than that of CO molecule adsorbed above Mn and S atoms, respectively, while the E_{Ad} of N_2 molecule adsorbed above Mn atom is 15.67 and 26.67 meV lower than that of N_2 molecule adsorbed above P and S atoms, respectively. Meantime, the E_{Ad} of NH_3 molecule adsorbed above P atom is 85.2 and 116.1 meV lower than that of NH_3 molecule adsorbed above Mn and S atoms, respectively. The E_{Ad} of NO molecule adsorbed above P atom is 7.5 and 26.4 meV lower than that of NO molecule adsorbed above Mn and S atoms, respectively. Furthermore, the E_{Ad} of NO_2 molecule adsorbed above Mn atom is 35.1 and 45.5 meV lower than that of NO_2 molecule adsorbed above P and S atoms, respectively. Thus, it is concluded that the most stable adsorption site for CO, NH_3, and NO is around P atom, while that for N_2 and NO_2 is near the Mn atom, based on the obtained E_{Ad} for CO, N_2, NH_3, NO, and NO_2 molecules adsorbed on $MnPS_3$ monolayer.

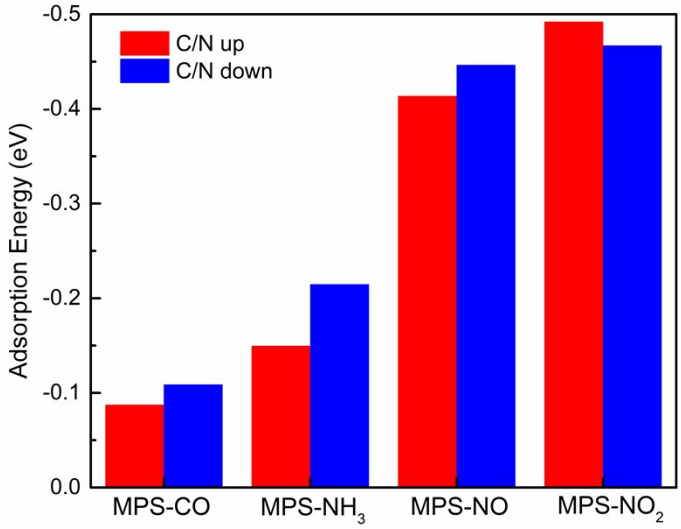

Fig.S1 Adsorption energy of MPS-CO, MPS-NH_3, MPS-NO, and MPS-NO_2 systems with different molecular orientation.

Due to the geometric asymmetry of CO, NH_3, NO and NO_2, the molecular orientation on MPS substrate are also tested. The adsorption energies of MPS-CO, MPS- NH_3, MPS-NO, MPS-NO_2 systems with different molecular orientation are calculated by Eq.1 in main text, and the obtained values are shown in Fig.S1. It can be found that the MPS-CO, MPS-NH_3, and MPS-NO systems with C/N atom pointing toward to the MPS substrate are more stable, while O atom pointing toward substrate is preferred for MPS-NO_2 system. Based on these stable structure, the magnetic properties and their origin would be studied in following sections.

Part 2. Magnetic ground state of MPS monolayer

To determine the ground state of MPS monolayer, systematic energy with four different magnetic configurations are calculated. The diagram of these four magnetic configurations including ferromagnetic (FM), Neél-antiferromagnetic (Neél-AFM), Zagzig-AFM and stripy-AFM are shown in Fig.S2. In Fig.S2, only Mn atoms are shown for a clear schematic, and the Mn atoms whose magnetic moments pointing up and down are represented by the red and green balls, respectively. According to DFT calculations, we find Neél-AFM owning the lowest energy is the ground state of MPS monolayer. Because it has been proved that the value of next-nearest exchange constant

J_2 in MPS monolayer is one order of magnitude lower than the nearest exchange constant J_1, so that we would focus on the nearest magnetic exchange coupling for MPS monolayer with and without molecular adsorption.

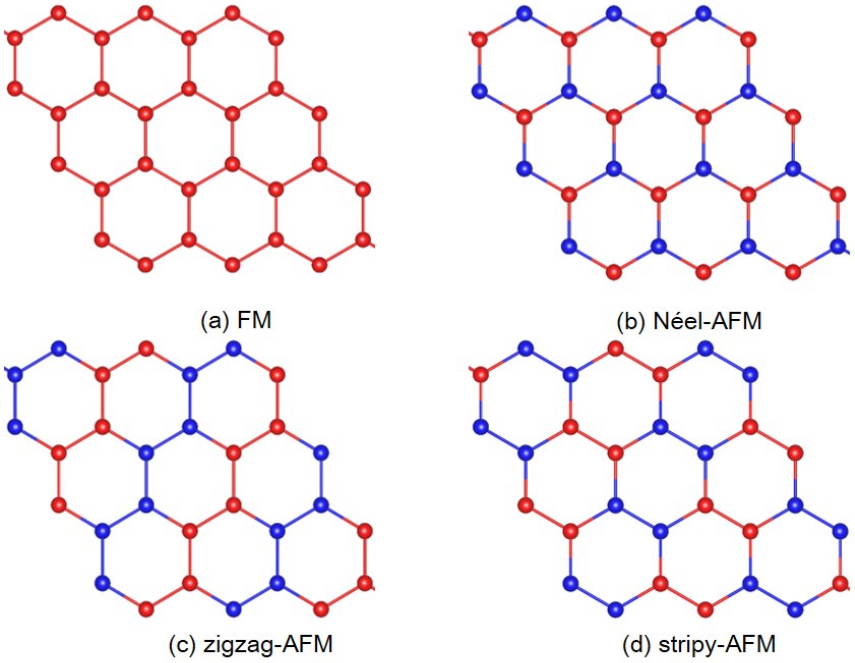

Fig.S2 The possible magnetic configurations of MPS monolayer, including ferromagnetic (FM) (a), Néel-antiferromagnetic (Néel-AFM) (b), Zigzag-AFM (c), and stripy-AFM (d). The red and blue balls represent the spin-up and spin-down Mn atoms.

Part 3. Calculating the magnetic exchange constants

To calculate the magnetic exchange constants between the *l*-th and *f*-th Mn ions, we need to gain the energy of MSP with and without molecular adsorption at four magnetic states. Consider the collinear spin orientations along the z-direction, four magnetic states are (1) $S_l^z = S_f^z = S$; (2) $S_l^z = S_f^z = -S$; (3) $S_l^z = S, S_f^z = -S$; (4) $S_l^z = -S, S_f^z = S$ and their energy can be expressed as:

$$\begin{aligned} E_1 &= E_0 + E_{\mathrm{EX}} + E_{\mathrm{SIA}}, \\ E_2 &= E_0 + E_{\mathrm{EX}} - E_{\mathrm{SIA}}, \\ E_3 &= E_0 - E_{\mathrm{EX}}, \\ E_4 &= E_0 - E_{\mathrm{EX}}. \end{aligned} \tag{S1}$$

Thus, J_{lf}^{zz} can be calculated by:

$$J_{lf}^{zz} = \frac{(E_1 - E_3) + (E_2 - E_4)}{4nZS^2} \tag{S2}$$

where n is the number of unit cell in supercell, Z is the coordination number. If the spin is set along x- or y- axis, J_{lf}^{xx} and J_{lf}^{yy} can also be calculated through

$$J_{lf}^{uu} = \frac{E_{ex}}{nZS^2}, \quad (u = x, y). \tag{S3}$$

In this paper, J_{lf}^{zz}, J_{lf}^{xx} and J_{lf}^{yy} of pristine MPS and MPS-molecule systems are evaluated. The difference between J_{lf}^{zz} and the average of J_{lf}^{xx} and J_{lf}^{yy} is defined as ΔJ_{lf}, which can reflect the strength of magnetocrystalline anisotropy.

Part 4 Calculating the asymmetric Dzyaloshinski-Moriya interaction parameters

As shown in Eq.(4), the asymmetric Dzyaloshinski-Moriya interaction parameters D_{lf}^x, D_{lf}^y, and D_{lf}^z are related to the noncollinear magnetic exchange coupling. D_{lf}^x can be gained by the energy difference between four states[1,2]: (1) $S_l^y = S_f^z = S$; (2) $S_l^y = S, S_f^z = -S$; (3) $S_l^y = S_f^z = -S$; (4) $S_l^y = -S, S_f^z = S$. Hence, D_{lf}^x can be written as

$$D_{lf}^x = \frac{\left(E_1 + E_4 - E_2 - E_3\right)}{4nZS^2}. \qquad \backslash^* \text{ MERGEFORMAT (S4)}$$

Similarly, D_{lf}^y and D_{lf}^z can also be gained by considering (1) $S_l^x = S_f^z = S$; (2) $S_l^x = S, S_f^z = -S$; (3) $S_l^x = S_f^z = -S$; (4) $S_l^x = -S, S_f^z = S$ and (1) $S_l^x = S_f^y = S$; (2) $S_l^x = S, S_l^y = -S$; (3) $S_l^x = S_f^y = -S$; (4) $S_l^x = -S, S_f^x = S$, respectively.

Part 5 Diagram of asymmetric exchange interactions in MPS

The diagram of asymmetric exchange interactions in MPS is presented in Fig.S3. According to the spin density distribution shown in Fig.3 in main text, the magnetism of MPS mainly originates from S and Mn atoms. So we don't show the P atoms in Fig.S4 for simplicity. The nearest-neighboring Mn ions around Mn_0 is remarked as Mn_1, Mn_2, and Mn_3, respectively.

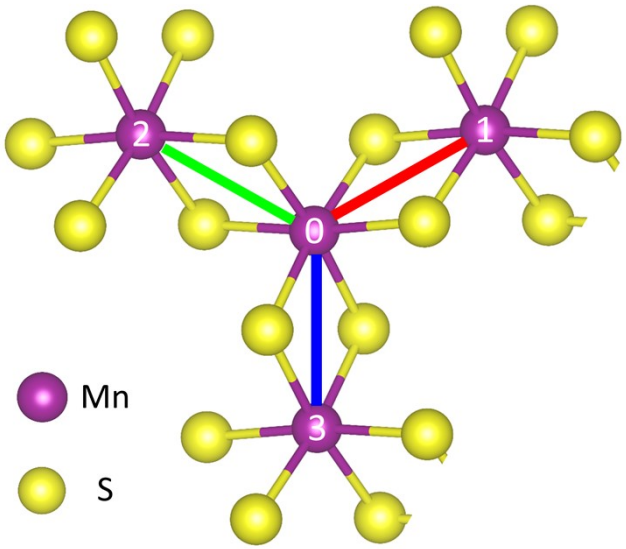

Fig.S3 Diagram of the asymmetric exchange interaction between Mn_0-Mn_1, Mn_0-Mn_2, and Mn_0-Mn_3 in pristine MPS.

Part 6 Charge density difference of adsorption system

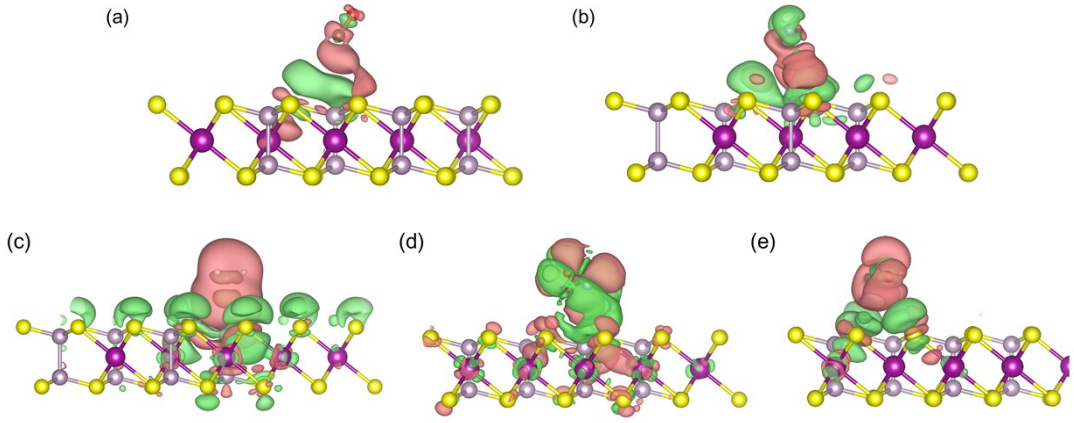

Fig.S4 Charge density difference of MPS-CO (a), MPS-N_2 (b), MPS-NH_3 (c), MPS-NO (d), and MPS-NO_2 (e), where the green and indianred isosurfaces represent the charge accumulation and charge dissipation, respectively.

The charge density difference for five adsorption systems is presented in Fig.S4, where the green and indianred isosurfaces are separated by $\pm 9 \times 10^{-5}$ e/Å^3. It is obvious that charge dissipation takes place around these gas molecules, while the charge accumulates on the top surface of MPS substrate. These results agree well with the charge transfer presented in Tab.1 in the main text.

Part 7. Diagram of Mn-S-Mn super-exchange coupling

The schematic representation of the Mn-S-Mn super-exchange coupling is shown in Fig.S5, where t_{2g} represents three-fold degenerate orbitals (d_{xy}, d_{xz}, and d_{yz}) and e_g represents two-fold degenerate orbitals (d_{z^2} and $d_{x^2-y^2}$). It can be observed from Fig.1 in main text that the nearest two Mn atoms (Mn_1 and Mn_2) are connected through an intermediate S atom with the Mn-S bond length of 2.04 Å and the Mn_1-S-Mn_2 angle of ~84º, allowing a Mn-S-Mn super-exchange interaction. The Néel-type AFM spin arrangement of MPS monolayer is determined by the half-filled t_{2g} and e_g orbitals and the spin density distribution (as shown in Figure 3).

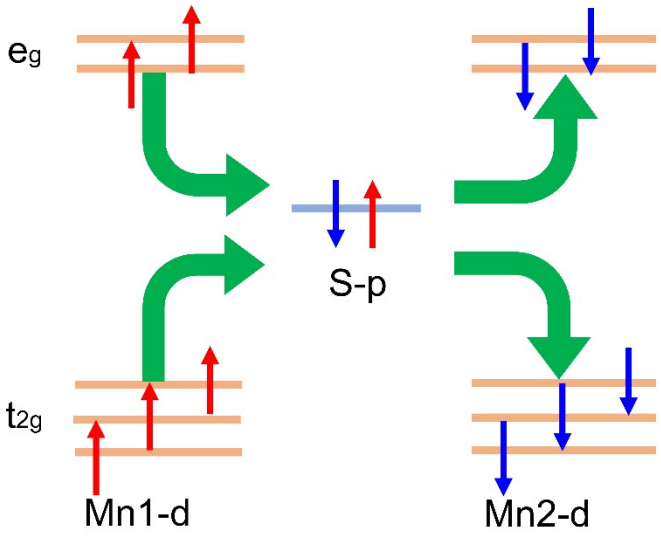

Fig.S5 Diagram of Mn-S-Mn super-exchange coupling in pristine MPS.

Part 8. Covalency between molecule and substrate

For the calculation of covalency between magnetic molecule and substrate, we present the partial DOSs of all adsorption systems in Fig.S6 where the Fermi level has been set as 0 eV. In the partial DOSs of MPS-NO and MPS-NO_2 systems, the impurity band shows larger spin splitting suggesting the gas molecule is magnetic, agreed well with the spin distribution in Fig.3 in main text. It is noted that the new super-exchange

coupling must occur between the magnetic molecule and Mn atoms in substrate, so only MPS-NO and MPS-NO_2 system are possible. Here, we calculated the covalency of Mn-gas-Mn super-exchange coupling in MPS-NO and MPS-NO_2 systems, and the obtained results are -2.329 and -9.82. As known, a larger covalency corresponds to a stronger super-exchange coupling, so that the super-exchange coupling between NO and Mn in MPS monolayer is much stronger than that in the MPS-NO_2 system.

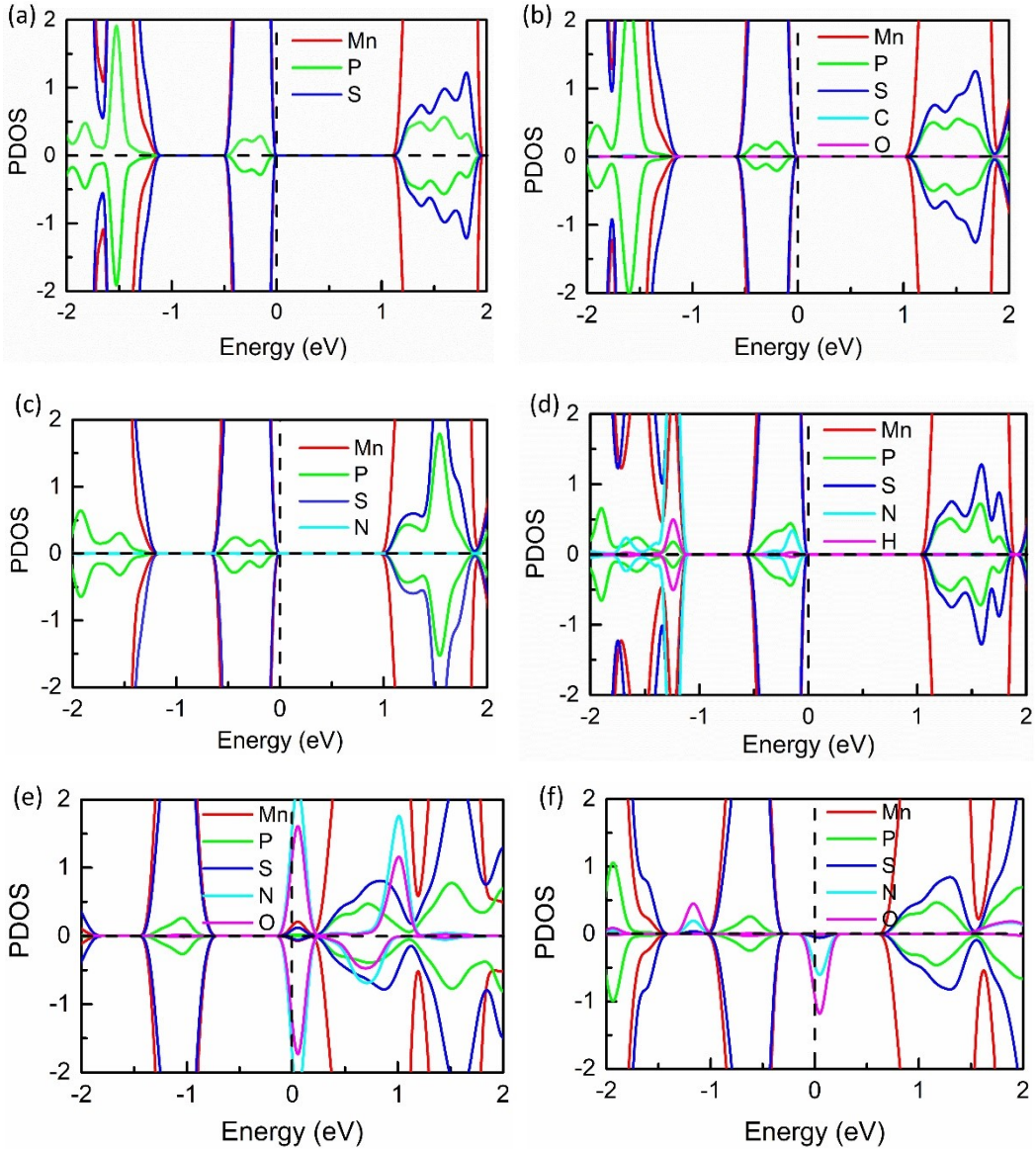

Fig.S6 Partial density of state (PDOS) of MPS (a), MPS-CO (b), MPS-N_2 (c), MPS-NH_3 (d), MPS-NO (e), and MPS-NO_2 (f).

References

1 Xiang, H., Lee, C., Koo, H.-J., Gong, X. & Whangbo, M.-H. Magnetic properties and energy-mapping analysis. *Dalton Transactions* **42**, 823-853, (2013).

2 Xiang, H. J., Kan, E. J., Wei, S.-H., Whangbo, M. H. & Gong, X. G. Predicting the spin-lattice order of frustrated systems from first principles. *Phys. Rev. B* **84**, 224429, (2011).